

Imaging the breakup of water molecule due to electron attachment

N Bhargava Ram*, V S Prabhudesai and E Krishnakumar

*W-140, Dept. of Nuclear and Atomic Physics,
Tata Institute of Fundamental Research,
1, Homi Bhabha Road, Mumbai 400005
Email: nbhargavram@tifr.res.in

Abstract

Using the velocity map imaging technique, we investigated the electron attachment resonances in water molecule at 6.5 eV, 8.5 eV and 12 eV in terms of the kinetic energy and angular distribution in the entire 2π range in the plane of the electron beam for H^- and O^- fragment ions. Unique angular distribution patterns together with kinetic energy data at the 8.5 eV and 12 eV resonances revealed dissociation dynamics for which axial recoil approximation breaks down. The most interesting dynamics is observed at the 12 eV resonance where we note selectivity in the dissociation of the two O-H bonds depending on the electron beam direction.

1. Introduction

The physical and chemical properties of negative ions are different from the corresponding neutral and cationic species as the nature of the potential experienced by the ‘extra electron’ in the anionic species is not always same as the valence electrons in neutrals and cations. Anions seldom have bound excited electronic states vis-a-vis neutrals and cations and this restricts the usage of optical spectroscopy techniques to study negative ions. Instead, they are studied *via* the negative ion resonance states (NIRS) formed in collisions of neutral atoms and molecules with low energy (<15 eV) electrons characterized by large cross sections or rate constants. These resonant states are essentially excited electronic states of the anion embedded in the detachment continuum corresponding to the neutral species and a free electron. Being unstable, the NIRS decays to a stable configuration. The dominant decay mechanism is to eject the extra electron leaving the atom or molecule in the neutral ground or excited state. This mechanism is known as autodetachment. However, in the case of molecules, the NIRS can also survive against autodetachment to dissociate into one or more neutrals

and a negative ion fragment. The latter process starting from the electron capture to fragmentation is called Dissociative Electron Attachment (DEA). Thus, the competition between the electronic relaxation mode and the nuclear relaxation mode determines the decay channel. In the DEA channel, measuring the fragment anion yield as a function of incident electron energy, one can identify the resonance energies and measure their cross sections. These cross sections for fragments of various masses identify the dominant decay channels, nature of the potential energy surface of the NIRS and its lifetime against autodetachment. Further, the measurements of kinetic energy and the angular distribution of the fragments are very important. The measurement of kinetic energy distribution helps to identify the dissociation products and the threshold energy of the process, while the angular distribution contains information of the electronic symmetry of the NIRS. The motivation behind this experimental work on studying dissociative electron attachment emanates from the discovery of the site selectivity in the process of electron attachment in our lab. It has been shown that selective fragmentation of C-H, N-H and O-H bonds in molecules are possible using

electron energy as a control parameter [1]. To understand this site selectivity in electron attachment process, we made systematic measurements on precursor molecules such as H_2O , H_2S , NH_3 , CH_4 and looked for signatures in bigger molecules containing similar bonds or functional groups containing these bonds. In this article, we describe the dissociation dynamics in water molecule due to low energy electron attachment, studied using the velocity imaging technique. The technique has given us unique and unprecedented level of details, which could not have been obtained by conventional setups with electrostatic analyzers limited by finite angular coverage (30° to 150°) and kinetic energy discrimination.

2. Experimental Setup

The most important parameters in unravelling the dynamics of the DEA process are the kinetic energy and angular distribution of the products and our objective is to measure them. For this we have developed an entirely novel ion momentum imaging technique [2] for low energy electron-molecule collisions. This has been inspired by the several charged particle imaging techniques, particularly the Velocity Map Imaging (VMI) technique, developed in recent times for a variety of collision experiments starting from photoionization, ionization by fast projectiles and photo-dissociation [3, 4].

The basic idea in VMI is that all the ions with the same velocity produced in a given interaction volume are mapped onto the same point on a two dimensional position sensitive detector (PSD). The image position on the PSD

and the time of arrival tell us about the all three velocity components of the anion fragments when they are formed. The imaging technique allows us to obtain the momentum distribution in the entire 2π range simultaneously. This makes it better and efficient as it is a single shot measurement of angular distribution and kinetic energy. There is also no kinetic energy discrimination of ions unlike many experimental setups reported in literature, where the energy analyzers are focused for ions at a particular energy.

Our experimental apparatus shown in Figure 1(a) consists of a magnetically collimated and pulsed electron beam that interacts with an effusive molecular beam formed by a capillary array. The negative ions formed in the interaction region are extracted into a time-of-flight mass spectrometer using a suitable extraction pulse after finite delay. The extraction field and the time-of flight tube along with a focusing electrode at the entrance of the flight tube provide the needed VMI condition. Figure 1(b) shows an ion trajectory simulation for the velocity focussing. The ions are detected using a two-dimensional position sensitive detector made of three 50 mm diameter micro-channel plates in Z-stack configuration and a Wedge and Strip anode. The ions striking the detector are recorded individually for their time of arrival (t) and position (x,y) in LIST mode using a CAMAC based data acquisition system running on 'LAMPS' software. We retrieve the angular distribution and kinetic energy distribution by choosing the central slice of the Newton sphere which contains the velocity distribution of the ions with respect to the electron beam direction is obtained by selecting a narrow time window during analysis.

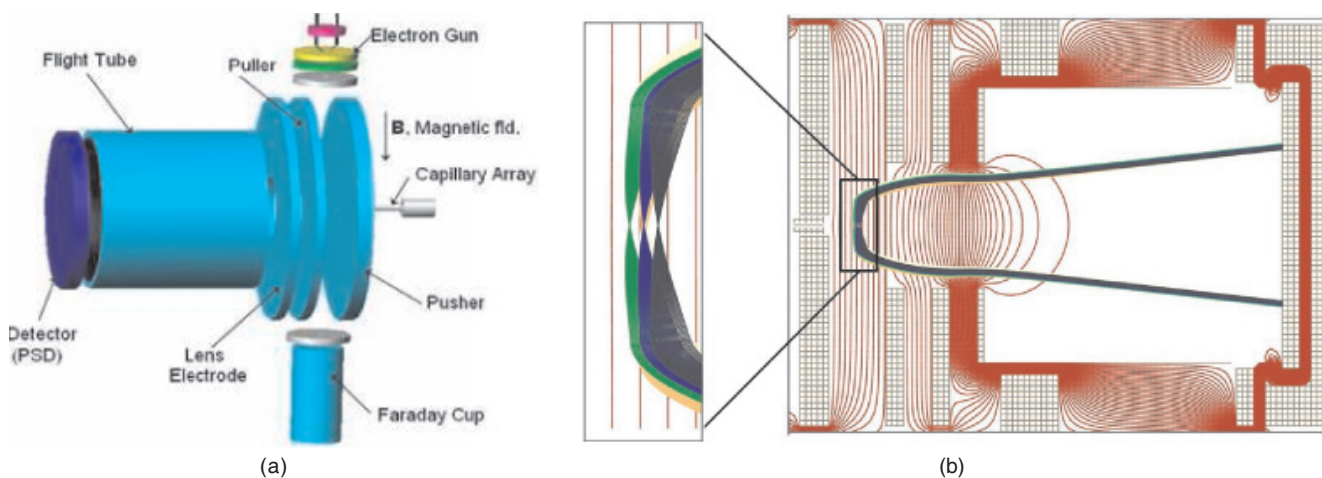


Figure 1. (a) Schematic of the VMI experiment setup for DEA studies (b) Ion trajectory simulations using SIMION showing the velocity focussing conditions for H^- ions of 4 eV with similar velocity distribution but different points of origin.

3. DEA in H₂O

Ours is the first experiment using ion momentum imaging to study the dissociation dynamics of anion resonances in water [5]. The study of anion resonances in water is of great significance as it is the most basic molecule of life and hence, very important that we know the details of its interaction with radiation and charged particles that produce ions and radicals and consequent chemical reactions involving them. Recent studies have highlighted the contribution of the DEA process in damage to DNA and its significance in radiation induced damage to biological tissues [6]. Added to this, the availability of *ab initio* theoretical calculations on electron attachment to water [7] makes detailed experimental studies on the dynamics of the DEA process a timely necessity.

Electron attachment to water occurs as resonances centered at 6.5, 8.5 and 11.8 eV and has been studied well to determine the exact resonance energies and widths, partial and absolute cross sections of the various anion fragments [8, 9]. The electronic ground state of water is $(1a_1)^2(2a_1)^2(1b_2)^2(3a_1)^2(1b_1)^2 \rightarrow {}^1A_1$ state (C_{2v} symmetry) and the three resonances are understood as ‘core excited Feshbach resonances’ where an extra electron is attached to the singly excited states (caused by the excitation of the $1b_1$, $3a_1$ and $1b_2$ electron respectively to $4a_1$) of the neutral water molecule leading to 2B_1 , 2A_1 and 2B_2 states respectively. The short lived H_2O^{*-} dissociates

to give H^- , O^- or OH^- fragments through various two-body and three-body channels as listed in Table 1. Even though formation of OH^- ions is favoured energetically, they are seen to be nearly absent and this is not understood.

Table 1. Electron attachment to H₂O: Possible dissociation channels with threshold energy

$H_2O + e^- \rightarrow H_2O^{*-} \rightarrow$	$H^- + OH (X {}^2\Pi) ;$	4.35 eV
	$H^- + OH^* (A {}^2\Sigma) ;$	8.38 eV
	$H^- + H + O ;$	8.75 eV
	$O^- + H_2 ;$	3.56 eV
	$O^- + H + H ;$	8.04 eV
	$OH^- ({}^2\Sigma) + H ;$	3.27 eV

4. Results and discussion

The velocity images of H^- and O^- ions from H_2O at the three resonances are shown in Figure 2. The electron beam direction is from top to bottom through the centre of every image. The radial distance from the centre of the image represents the magnitude of the velocity of the ions when they are formed. Thus, the images give differential cross sections in both energy and angle.

First resonance at 6.5 eV: The H^- ions produced from the first resonance process (as seen in Figure 2(a)) are ejected almost perpendicular to the electron beam direction with a continuous distribution of intensity along the radial direction which appear to increase with radius.

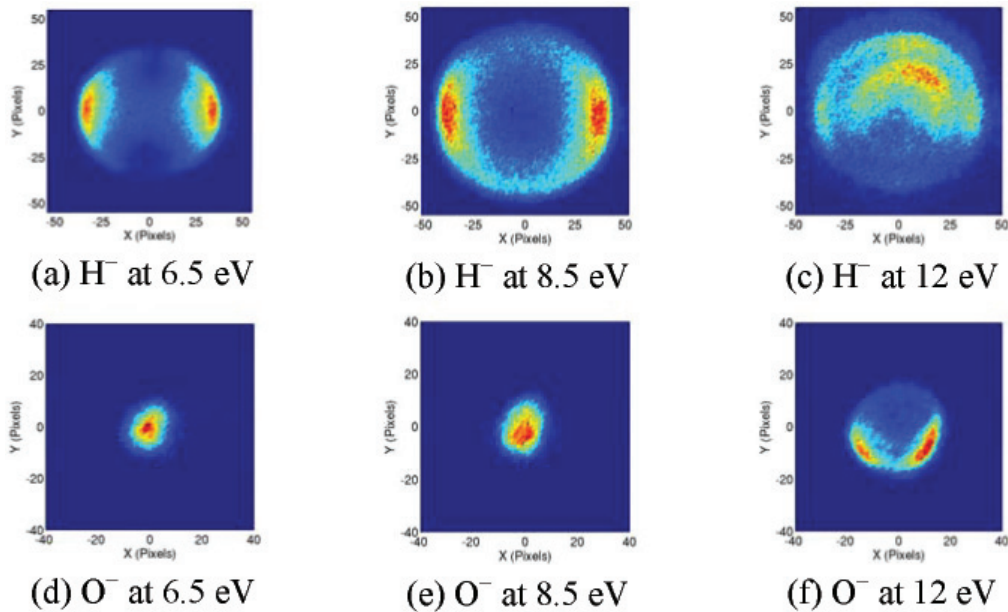


Figure 2. Velocity Images of H^- and O^- at the three resonances.

The kinetic energy of H^- ions range from 0 to about 2.5 eV with a peak at 1.8 eV and is attributed to the $H^- + OH$ channel with threshold energy 4.35 eV. The broad KE distribution is an indication of vibrational (upto $v=4$ states) and rotational excitation of the OH fragment. The intensity distribution for H^- appears to peak at an angle of about 100° with respect to the electron beam direction and is consistent with earlier measurements [10, 11]. The excellent fit obtained for B_1 symmetry using p and d partial waves by us reiterates the previous assignment of B_1 symmetry to this resonance. The velocity image of O^- at 7 eV (Figure 2(d)) shows a small blob suggesting very little kinetic energy. We find the dissociation channel to be $O^- + H_2$ (threshold: 3.56 eV).

Second resonance at 8.5 eV: At the second resonance at 8.5 eV, the projectile electron attaches to the $(3a_1)^{-1} (4a_1)^{-1}$ excited state of the neutral water molecule and forms a H_2O^* anion of 2A_1 symmetry. The velocity images of H^- and O^- arising from this resonance are shown in Figure 2 (b) and (e) respectively. H^- is seen to be produced via the $H^- + OH ({}^2\Pi)$ channel same as in the first resonance process with enhanced internal excitation of the OH fragment. The angular distribution shows scattering intensities peaking in the 90° direction with finite intensity in other directions too. This was however not in agreement with a previous measurement by Belic *et al.* [11] who reported an angular distribution with peaks at 45° and 135° in accordance with A_1 symmetry whereas our data seemed to suggest B_1 symmetry. However, detailed

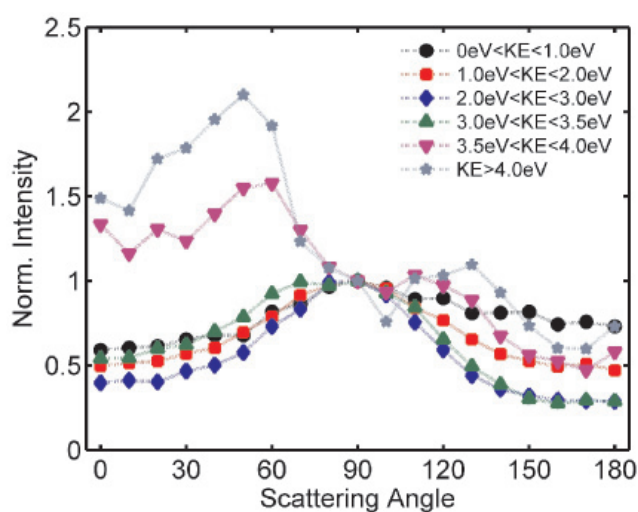


Figure 3. Variation of angular distribution of H^- ions as a function of kinetic energy at the 8.5 eV resonance depicting breakdown of axial recoil dynamics.

analysis shows that the angular distribution of H^- varies with its kinetic energy as shown in Figure 3. H^- ions with maximum KE showed angular distribution consistent with A_1 symmetry whereas ions with lower KE showed characteristics of B_1 symmetry. This is due to the fact that the H_2O^* molecular negative ion at 8.5 eV once formed undergoes structural changes due to bending mode vibrations before the dissociation could take place, thereby distorting the angular distributions.

Thus, what we learn is, when the dissociation is fast enough before the molecule could undergo structural changes, most of the excess energy is pooled into the kinetic energy and consequently, the angular distribution of the H^- ions with maximum kinetic energy retains the orientation of the dissociating O-H bond with respect to the electron beam and commensurate with the A_1 symmetry for the resonance. Thus in this case, the axial recoil approximation is held. The production of low kinetic energy H^- ions indicate that part of the excess energy is distributed into excitation of the second O-H bond and the dissociation process is slower. It appears that unlike in the case of the 6.5 eV resonance, the potential energy surface of the 8.5 eV resonance favours strong bending mode excitation as well. Thus any time delay in the dissociation would also lead to bending mode vibration and subsequently the H^- ions formed with lower kinetic energy will have differing angular distributions as manifested in our measurements. O^- ions (Figure 3(e)) again seen as a blob with very little energy at this resonance and are formed entirely by a three-body fragmentation – $O^- + H + H$ with threshold 8.04eV.

Third resonance process at 12 eV: The velocity images of H^- ions from the third resonance (Figure 2(c) and (f)) process at 12 eV show three clear rings in the backward hemisphere corresponding to three different dissociation pathways of the molecular negative ion i.e. $H^- + OH(X {}^2\Pi)$ (outermost ring), $H^- + OH^*(A {}^2\Sigma)$ (middle ring) and $H^- + H + O$ (innermost ring) and also inferred as three distinct structures in the kinetic energy distribution (Figure 4(a)). It is for the first time all the three channels are observed.

The angular distribution as seen from the images appears to be very unique with the H^- being ejected predominantly in the backward hemisphere. In contrast, the O^- is ejected mostly in the forward hemisphere via the

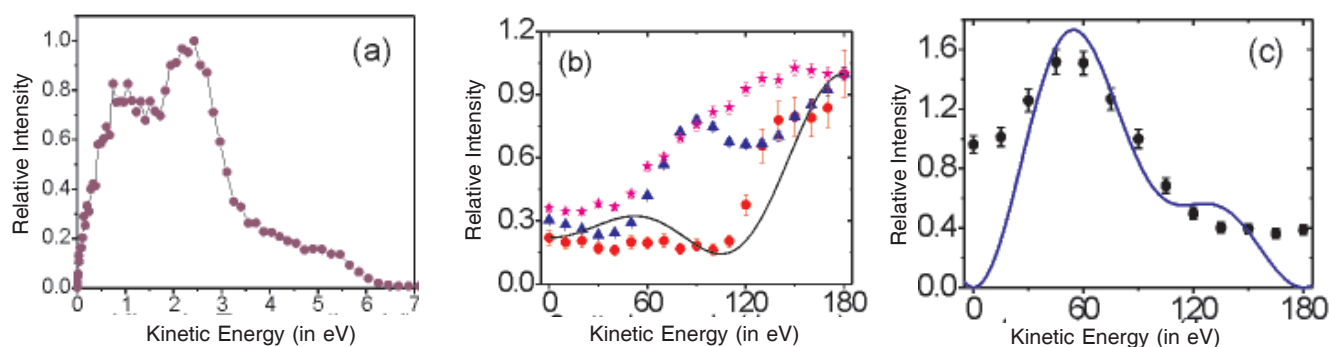


Figure 4. (a) KE distribution of H^- ions at 12 eV resonance. (b) Angular distribution of H^- at 12 eV from water (normalized at 180°): (•) outer ring (▲) middle ring and (*) inner ring (b) Angular distribution of O^- at 12 eV. The curves represent best fits for B_2 symmetry using p and d partial waves under axial recoil approximation.

$\text{O}^- + \text{H} + \text{H}$ channel. A detailed analysis of the kinetic energy distribution shows the presence of sequential fragmentation through an intermediate OH^* state in both the three-body break up channels leading to H^- and O^- formation. The angular distributions of the ions at the third resonance are given in Figure 4(b) and (c) along with the fits using the lowest possible partial waves, p and d for a B_2 resonance under axial recoil approximation. We find that the fit is reasonably good for the $\text{H}^- + \text{OH}$ ($X^2\Pi$) channel, which has the maximum kinetic energy release, while those of the other two channels, $\text{H}^- + \text{OH}$ ($A^2\Sigma$) and the $\text{H}^- + \text{O} + \text{H}$ are markedly different and do not agree with the fit (Figure 4(b)). It is seen that the overall angular distribution from being strongly in the backward direction for the OH ($X^2\Pi$) channel tend to become increasingly smoothed for the other two channels, with decreasing H^- energy. The angular distribution for the OH ($X^2\Pi$) channel shows that the electron is approaching along the H-O bond and that mostly this particular O-H bond is being broken. This behaviour shows that even within the two O-H bonds, there is selectivity for bond breaking depending on whether it is oriented toward the electron beam or not. We interpret this selectivity as due to excitation of asymmetric stretch vibration along that bond during the time of the electron capture process itself. The behaviour of the angular distributions in the two inner rings may be explained in terms of the structural changes that the molecular negative ion is undergoing after electron capture. For the outermost ring, the H^- has the largest possible kinetic energy and we expect the dissociation to be the fastest and mostly follow the axial recoil approximation. For the middle ring corresponding to the OH ($^2\Sigma$) channel, the H^- energy is

considerably reduced to 2.5 eV due to the electronic and vibrational excitation of the OH. The vibrational motions of the molecule could force fragmentation to take place along the other O-H bond oriented nearly at 90° to the electron beam. In the case of the three-body fragmentation channel, the bending mode vibration appears to smoothen out the anisotropy further. The sequential fragmentation present in this channel will also smooth the angular distribution. For the formation of O^- , both the OH bonds need to be broken and one can deduce the angular distribution of O^- using the axial recoil approximation if the role of vibrations and rotations are neglected. Such comparison of the angular distribution is shown in Figure 4(c). The difference between the fit and the observed distribution in the case of O^- is due to deviation from the axial recoil approximation, including sequential fragmentation.

5. Conclusion

To conclude, the DEA dynamics in water are unravelled in terms of the strong anisotropy in the angular distribution of the fragment negative ions. We observe signatures of breakdown of axial recoil based dissociation at the 8.5 eV and 12 eV. Bending mode vibrations cause a crossover from A_1 symmetry to B_1 at the 8.5 eV resonance. At 12 eV resonance, we observe four dissociation channels, including three body fragmentation leading to H^- and O^- ions. We identify selectivity in dissociation of the two O-H bonds for this resonance depending on the direction along which the electron is approaching. The three less energetic dissociation channels also show strong deviation from axial recoil approximation.

References

- [1] V. S. Prabhudesai, D Nandi, A Kelkar and E Krishnakumar, *Phys. Rev. Lett.* **95**, 143202 (2005)
- [2] D. Nandi, V S Prabhudesai and E Krishnakumar, *Rev. Sci. Instrum.* **76**, 053107 (2005)
- [3] Benjamin Whitaker (edt.), *Imaging in Molecular Dynamics: Technology and Applications* (Cambridge University Press, 2003)
- [4] J. Ullrich et al., *J.Phys.B. Topical Review* **B30**, 2917 (1997)
- [5] N Bhargava Ram, V S Prabhudesai and E Krishnakumar, *J. Phys. B: At. Mol. Opt. Phys.*, **42**, 225203 (2009)
- [6] B Boudaïffa, P Cloutier, D Hunting, M A Huels, L Sanche, *Science*, **287**, 1658 (2000)
- [7] D J Haxton, Z Zhang, C W McCurdy and T N Rescigno, *Phys. Rev. A*, **69**, 062713 (2004) ; *Phys. Rev. A*, **69**, 062714 (2004); *Phys. Rev. A*, **72**, 022705(2005) ; *Phys. Rev. A*, **73**,062724 (2006) ; *Phys. Rev. A*, **75**, 012710 (2007) ; *Phys. Rev. A*, **75**, 012711 (2007); *Phys. Rev. A*,**78**, 040702(R) (2008)
- [8] J Fedor et al., *J. Phys. B : At. Mol. Opt. Phys.*, **39**, 3935 (2006)
- [9] P Rawat, V S Prabhudesai, G Aravind, M A Rahman and E Krishnakumar, *J. Phys. B: At. Mol. Opt. Phys.*, **40**, 4625 (2007)
- [10] S Trajmar and R I Hall, *J. Phys. B: At. Mol. Phys*, **7**, L485 (1974)
- [11] D S Belic, M Landau and R I Hall, *J. Phys. B: At. Mol. Phys*, **14**, 175 (1981)



N. Bhargava Ram did his B. Sc. from Ferguson College, Pune in the year 2004 and M. Sc in Physics (by thesis) from TIFR, Mumbai in May 2007. He obtained his Ph. D. degree in Physics from the same institute in June 2010. His research interests are in the dissociation dynamics of molecular anions, ion imaging techniques, excited state of molecules, molecular spectroscopy and quantum optics. He has many publications in journals of international repute. Bhargava Ram won the First Best Award in YPC 2010.